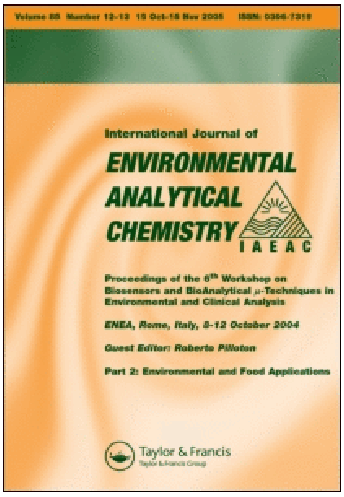

International Journal of Environmental Analytical Chemistry
Publication details, including instructions for authors and subscription information:
http://www.informaworld.com/smpp/title~content=t713640455

SPICE modelling and design optimization of micropumps

Elisa Morganti[a]; Iolanda Fuduli[a]; Andrea Montefusco[a]; Marco Petasecca[a]; Giorgio U. Pignatel[a]
[a] Università di Perugia, DIEI, 06125 Perugia, Italy

To cite this Article Morganti, Elisa , Fuduli, Iolanda , Montefusco, Andrea , Petasecca, Marco and Pignatel, Giorgio U.(2005) 'SPICE modelling and design optimization of micropumps', International Journal of Environmental Analytical Chemistry, 85: 9, 687 — 698

To link to this Article: DOI: 10.1080/03067310500153876

URL: http://dx.doi.org/10.1080/03067310500153876

Intern. J. Environ. Anal. Chem.
Vol. 85, Nos. 9–11, 10 August–15 September 2005, 687–698

Taylor & Francis
Taylor & Francis Group

SPICE modelling and design optimization of micropumps

ELISA MORGANTI*, IOLANDA FUDULI, ANDREA MONTEFUSCO,
MARCO PETASECCA and GIORGIO U. PIGNATEL*

Università di Perugia, DIEI, via G. Duranti 93, 06125 Perugia, Italy

(*Received 8 November 2004; in final form 15 February 2005*)

This article describes a study concerning micropump design for medical purposes. In particular the project is focused on treatment of Hydrocephalus. An actuator glued on a membrane, a pumping chamber and a certain number of valves constitute the micropumps. The actuator is a piezoelectric disc, controlled according to data collected by means of a pressure sensor. We have studied two different structures of micropump: the first with membrane valves, and the second with diffuser/nozzle valves, without moving parts. Modelling both micropumps with electrical equivalent networks, we are able to estimate the pump behaviour, in terms of flow rate, with a simulator such as SPICE, and to optimize the micropump design for best performances.

Keywords: μ-Systems; MEMS; μ-Fluidics; Hydrocephalus

1. Introduction

Piezoelectric micropumps are attractive devices because they can achieve relatively high flow rates in small dimensions. The aim of this work is to investigate the feasibility of micromachined micropumps performing flow rates up to $2000\,\mu L\,s^{-1}$ with dimensions not exceeding $0.2 \times 0.5 \times 2\,cm^3$ as determined by the medical purpose for which they are assigned.

First, we have analysed two different micropump designs taken from the literature from which we have extracted equivalent electric networks with lumped elements. Then these networks have been modelled with commercial EDA-CAD software (SPICE). Second, we have tried to optimize the pump's performance to achieve the desired specifications.

2. Modelling

The first micropump we have studied is shown with membrane valves, as proposed by Bohm [1] (see figure 1). It exhibits a flow-rate of $35\,\mu L\,s^{-1}$ at a frequency of about 100 Hz.

*Corresponding authors. Fax: +39-075-585-3654. Email: winnie@diei.unipg.it; pignatel@diei.unipg.it

International Journal of Environmental Analytical Chemistry
ISSN 0306-7319 print: ISSN 1029-0397 online © 2005 Taylor & Francis
DOI: 10.1080/03067310500153876

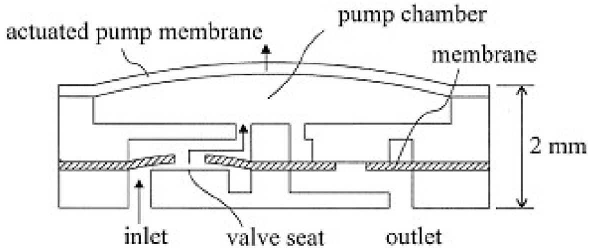

Figure 1. Micropump with membrane valves [1].

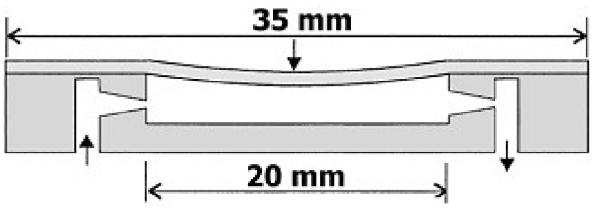

Figure 2. Micropump with diffuser valves [2].

The second design is a micropump with valves that have no moving parts, i.e. nozzle/diffuser valves, as described by Ullmann [2] (see figure 2). This pump has a flow-rate of $28\,\mu L\,s^{-1}$ at a resonant frequency of about 550 Hz.

In order to model these micro-fluidic systems we have used the analogy with electrical systems and in particular the evident formal similarity between the equations governing the pressure (P) of a fluid mechanical system and those governing the voltage (e) of an electrical series RLC circuit:

$$P = \frac{m}{S^2}\frac{d\phi}{dt} + \left(\frac{\beta}{S^2}\right)\phi + \left(\frac{k}{S^2}\right)\int \phi\, dt \tag{1}$$

$$e = L\frac{di}{dt} + Ri + \frac{1}{C}\int i\, dt \tag{2}$$

We can define a correspondence between the different terms of both equations as [3]:

$$L \Rightarrow \frac{m}{S^2} \qquad R \Rightarrow \frac{\beta}{S^2} \qquad C \Rightarrow \frac{S^2}{k} \tag{3}$$

In these equations, m is the mass, β the friction coefficient, k the spring constant, S the surface and ϕ the flow rate in a fluidic system; L is the inductance, R the resistance, C the capacitance and I the current in an RLC circuit.

We can use the analogy between the laws that rule the behaviour of the two systems to build equivalent networks of the microfluidic components. In this way, microfluidic devices can be analysed with the same means we use in electronics because their components will be simply represented by a circuit made of resistors, capacitors and inductors.

We can define a hydraulic resistance (R_{hyd}) which represents the energy dissipation due to the effect of the fluid's viscous friction against the component's walls.

The relation obtained is similar to Ohm's law:

$$\Delta P = R_{\mathrm{hyd}}\phi \tag{4}$$

The inductive behaviour is given by the inertial term. The hydraulic inertance (I_{hyd}) represents the effect of a certain mass that is accelerated in the device; it can be both due to the fluid that moves in the component, or to a part of the device itself that moves, such as a membrane or a cantilever. It is similar to Newton's relation $f = ma$:

$$\Delta P = I_{\mathrm{hyd}} \frac{\mathrm{d}\phi}{\mathrm{d}t} \tag{5}$$

The hydraulic capacitance (C_{hyd}) represents the elastic behaviour of the microfluidic component; it links pressure difference to volume variation:

$$C_{\mathrm{hyd}} = \frac{\mathrm{d}V}{\mathrm{d}P} \tag{6}$$

This variation is due both to the deformation of the structure and the elastic property of the fluid.

We obtain the relation:

$$\phi = C_{\mathrm{hyd}} \frac{\mathrm{d}P}{\mathrm{d}t} \tag{7}$$

Table 1 shows a comparison between microfluidic and electrical quantities. To obtain the correspondent unity we can simply change coulombs to cubic meters.

Thanks to these equations we can find the electrical equivalent network of each element of the micropump [4]. We show equations only for micropump with diffuser valves. Geometrical dimension of both micropumps are shows in tables 2 and 3.

Tubes (see figure 3) can be represented with a simple equivalent network in which the resistor is associated with the friction effect of the fluid flowing, the inductor to its dynamic inertia and the capacitor to its elasticity.

$$R = \frac{8\mu l}{\pi a^4} = 3.88 \times 10^8\,\mathrm{N\,s\,m^{-5}} \tag{8}$$

$$I = \frac{\rho l}{S} = 39.4 \times 10^6\,\mathrm{N\,s^2\,m^{-5}} \tag{9}$$

$$C = \frac{V}{K} = 1.15 \times 10^{-16}\,\mathrm{m^5\,N^{-1}} \tag{10}$$

All terms in these equations have already been introduced in tables 2 and 3.

Table 1. Comparison between microfluidic and electrical domains.

Microfluidic			Electrical		
Pressure	P	$\mathrm{J\,m^{-3}}$	Voltage	V	$\mathrm{J\,C^{-1}}$
Flow	ϕ	$\mathrm{m^3\,s^{-1}}$	Current	I	$\mathrm{C\,s^{-1}}$
Resistance	R_{hyd}	$\mathrm{J\,s\,m^{-6}}$	Resistance	R	$\mathrm{Js\,C^{-2}}$
Inertance	I_{hyd}	$\mathrm{J\,s^2\,m^{-6}}$	Inductance	L	$\mathrm{Js^2\,C^{-2}}$
Capacitance	C_{hyd}	$\mathrm{m^6\,J^{-1}}$	Capacitance	C	$\mathrm{C^2\,J^{-1}}$

Table 2. Geometrical dimension of micropump with diffuser valves.

Elements	Symbol	Value
Membrane radius	a	5 mm
Membrane thickness	h	0.15 mm
Cosinusoidal flexion	γ	0.297
Young's modulus steel	E	190 GPa
Poisson's steel	ν	0.33
Steel density	ρ	$7850\,\mathrm{kg\,m^{-3}}$
Actuator density	ρ	$7000\,\mathrm{kg\,m^{-3}}$
Actuator radius	a	5 mm
Actuator thickness	h	0.2 mm
Pump chamber depth	h_c	0.2 mm
Pump chamber radius	a	5 mm
Valves efficiency	ε	0.18
Valves length	d	4.2 mm
Minimum diameter valves	$h_m(0)$, $w_m(0)$	0.15 mm
Average diameter valves	h_m	0.29 mm
Tube length	$2l$	1.8 mm
Water coprimibility	K	2.2 GPa
Water density	ρ	$1000\,\mathrm{kg\,m^{-3}}$
Water viscosity	μ	$0.001\,\mathrm{m^2\,s^{-1}}$

The membrane has both an inductive and capacitive effect. The first is related to its inertia when moving; the capacitor represents its deformation with the consequent volume variation.

An actuator applies a pressure to the system; this is equivalent to applying a voltage to a node of the network and it can simply be represented by a voltage source (see figure 4):

$$k = \frac{64}{12(1-\nu^2)}\frac{\gamma\pi E h^3}{a^2} = 1.43\times 10^5\,\mathrm{N\,m^{-1}} \tag{11}$$

$$C_{\mathrm{membrane}} = \frac{(\gamma S)^2}{k} = 3.8\times 10^{-15}\,\mathrm{m^5\,N^{-1}} \tag{12}$$

$$m_{\mathrm{Eff}} = \gamma(m_{\mathrm{membrane}} + m_{\mathrm{actuator}}) = 53.46\times 10^{-6}\,\mathrm{kg} \tag{13}$$

$$I_{\mathrm{membrane}} = \frac{m_{\mathrm{Eff}}}{(\gamma S)^2} = 34.7\times 10^3\,\mathrm{N\,s^2\,m^{-5}} \tag{14}$$

The pump chamber (see figure 5) is relatively wide, compared to tubes, so friction effects are not considered in its equivalent network. It only has an inductor and

Table 3. Geometrical dimension of micropump with membrane valves.

Membrane radius	a	5 mm
Membrane thickness	h	0.075 mm
Cosinusoidal flexion	γ	0.297
Young's modulus brass	E	110 Gpa
Poisson's brass	ν	0.34
Brass density	ρ	8600 kg m^{-3}
Actuator density	ρ	7000 kg m^{-3}
Actuator radius	a	5 mm
Actuator thickness	h	0.2 mm
Pump chamber vol.	V_c	1 μL
Water coprimibility	K	2.2 Gpa
Water density	ρ	1000 kg m^{-3}
Water viscosity	μ	0.001 m^2 s^{-1}

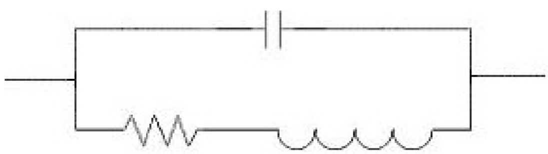

Figure 3. Tube's equivalent network.

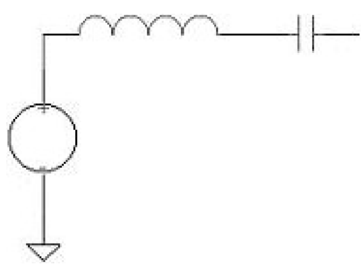

Figure 4. Membrane and actuator's equivalent network.

a capacitor representing the inertia and compressibility of the fluid in the chamber, respectively:

$$C_{\text{camera}} = \frac{Sh_c}{K} = 7.136 \times 10^{-18} \text{m}^5\,\text{N}^{-1} \tag{15}$$

$$I_{\text{camera}} = \frac{\rho h_c}{S} = 2.55 \times 10^3\,\text{Ns}^2\,\text{m}^{-5} \tag{16}$$

Valves have a different behaviour in 'forward' and 'reverse' conditions; their equivalent network is divided into two branches, the ideal diodes selecting which one works. Each branch is obtained by analysing the valve's behaviour in each condition: one represents the conduction and the other the leakage.

Mechanical valves have elastic moving parts such as cantilevers or membranes (see figure 6) that give a capacitive effect, represented in each branch by a capacitor. The resistor represents the effect of the viscous friction of the fluid passing through the valve.

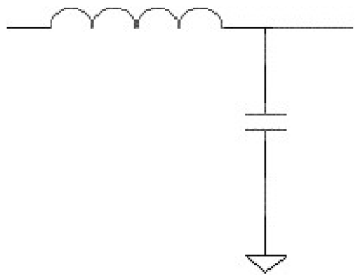

Figure 5. Pump chamber's equivalent network.

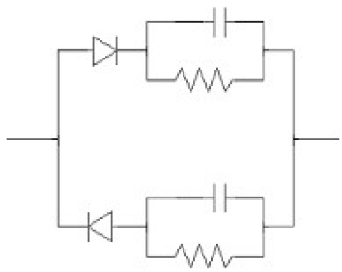

Figure 6. Mechanical valve's equivalent network.

In the 'forward' or 'conduction' condition, a little resistance R_+ allows the fluid to flow easily and a big capacitance models the elasticity of the mechanical parts that widely bend to open a passage to the fluid. In the 'reverse' or 'leakage' condition, we have a bigger resistance R_- because of the shutting down of the valves, and a little capacitance due to small deflections of the moving part pushed against its base.

Inductive effect is not considered as long as the weights of the moving structure and the fluid contained in the valve is small compared to that contained in the tubes and in the pump chamber.

In non-mechanical valves (see figure 7) such as the nozzle/diffuser types, there are no moving parts so no capacitive effect is considered. Instead, a considerable mass of fluid is moving through it and its inertial effect is represented by an inductor.

In this case, R_+ and R_- are not very different as long as there are no mechanical obstacles to the fluid flow in the 'reverse' condition. The directing effect is due to turbulences inside the valve:

$$R_+ = \frac{8\mu}{\pi} \int \left(\frac{1}{h_v(x)} + \frac{1}{w_v(x)} \right)^4 \mathrm{d}x = 55 \times 10^9 \,\mathrm{Ns\,m^{-5}} \tag{17}$$

$$I_+ = \rho \int \frac{\mathrm{d}x}{h_v(x) w_v(x)} = 6.19 \times 10^4 \,\mathrm{Ns^2\,m^{-5}} \tag{18}$$

$$R_- = \frac{1-\varepsilon}{1+\varepsilon} R_+ = 1.27 R_+ = 70 \times 10^9 \,\mathrm{Ns\,m^{-5}} \tag{19}$$

$$I_- = \frac{1-\varepsilon}{1+\varepsilon} I_+ = 1.27 I_+ = 7.9 \times 10^4 \,\mathrm{Ns^2\,m^{-5}} \tag{20}$$

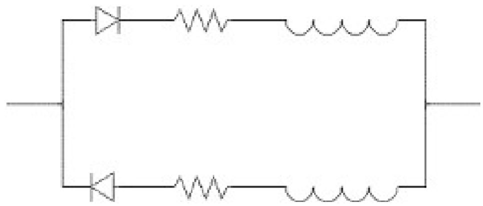

Figure 7. Diffuser valve's equivalent network.

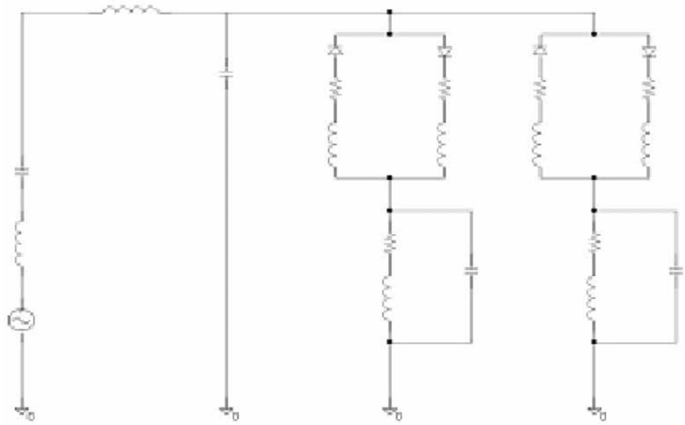

Figure 8. Equivalent network of a diffuser micropump.

All the circuit elements shown in the previous figures were used to build the equivalent networks of the micropumps reported [1, 2].

The equivalent network built for the micropump with diffuser valves [2] is illustrated in figure 8.

An analogue network was obtained for the micropump with membrane valves reported in [1].

After simulating both circuits with SPICE we have found that the maximum flow rate of the pump reported in [1] (see figure 9) is slightly overestimated, although correct frequency dependence is indicated (see figure 10).

The flow rate of the circuit, reported in figure 8, is instead reproduced very well in figure 11 and a good match with the experimental data reported in [2] is shown.

3. Design optimization

After having studied the two types of micropump, we have attempted to modify the design parameters with the aim of increasing the maximum flow-rate. A first analysis on the effects of increasing the size of the elements is made. Size can be varied as long as the structural strength is not compromised. In other words, moving parts that sustain a certain mechanical stress such as membranes must not break if their

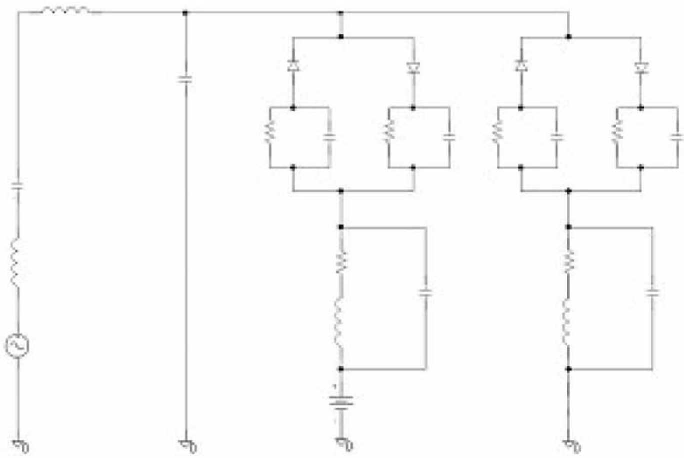

Figure 9. Equivalent network of a membrane micropump.

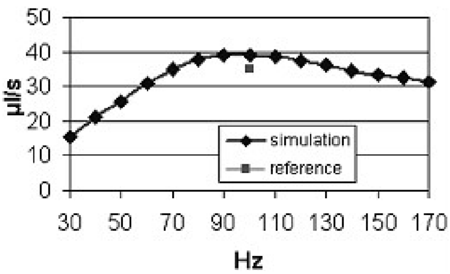

Figure 10. Flow-rate simulation and reference of plastic micropump [1].

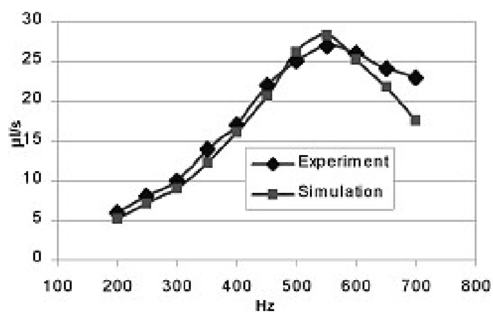

Figure 11. Flow-rate comparison between simulation and experiment of the diffuser micropump [2].

size is changed. This is possible if the mechanical stress in the membrane is maintained below the maximum value of the fracture stress limit σ_f [5]:

$$\sigma_f \propto P \frac{\text{radius}^2}{\text{thickness}^2} = \text{cost} \tag{21}$$

To avoid a break we have to find a compromise between increasing pressure, size of the membrane and its thickness. This rule gives us a criterion to understand the effects of a size variation. Using α as the linear scaling factor, we can say, as a first approximation, that capacitances are scaled by α^3 and inertances by α^{-1}. We note that the performance, in terms of maximum flow rate is not affected by this; only reactive effects due to the change of capacitive and inductive loads values are obtained such as a shift of the resonant frequency of the micropump.

Another possibility to increase the pump flow-rate is to increase the pressure developed by the system membrane actuator. To do this, we could increase the thickness of the membrane in agreement with equation (7). In addition, the magnitude of pressure cannot be arbitrary; for biomedical applications it must satisfy a biocompatibility condition.

Following these considerations, we concentrate our attention on the characteristics of the valves. In principle, increasing the dimensions of the valve determines a significant lessening of the hydraulic resistance and therefore an increase of the flow-rate. Anyway, valve behaviour is strongly non-linear and the geometry complex can be considered only as a first guess, while trying to understand the effect of a size scaling on their resistance with simple considerations.

In this case we considered the valve as a simple tube with an obstacle, like a bottleneck, and saw that in the first approximation its resistance changed by α^{-3}.

The capacitive and inductive loads of valves are obtained by similar considerations to those made for membranes and tubes.

However, if we define the valve rectification efficiency as [6]:

$$\varepsilon = \frac{R_+ - R_-}{R_+ + R_-} \tag{22}$$

where R_+ and R_- is the forward and backward valve resistance respectively, and calculate the valve-tube system efficiency, we obtain:

$$\varepsilon_{\text{series}} = \frac{R_+ - R_-}{R_+ + R_- + 2R_{\text{tube}}} \tag{23}$$

In nozzle/diffuser valves R_+ and R_- have the same order of magnitude so that their efficiency is very low (<0.3). In order to find a compromise between maximum efficiency and minimum resistance we calculated the total flow rate φ_{tot}, as a function of R_- and ε.

To fix a value for R_{tube}, we indicate with β the ratio between R_- and R_{tube}. We can see in figure 12 the dependence of φ_{tot} *versus* β at different values of ε for the micropump with diffuser valves. A maximum is obtained for $R_- \approx 1.2R_{\text{tube}}$ with $\varepsilon = -0.3$.

The efficiency of mechanical valves is usually much higher than that of nozzle/diffuser valves, and in ideal conditions it can approximate unity; R_- is very high, in this case, we define β' as the ratio between R_+ and R_{tube}.

Calculating again the total flow φ_{tot} *versus* β', the resulting plot is reported in figure 13 for values of ε increasing from 0.96 to 1.

The diagram shows that, even for efficiency values very close to unity, a remarkable decrease of valve efficiency may occur if the valve resistance is not properly matched with the tube resistance. A maximum is shown for $R_+ \approx 0.13R_{\text{tube}}$ with $\varepsilon = 0.96$.

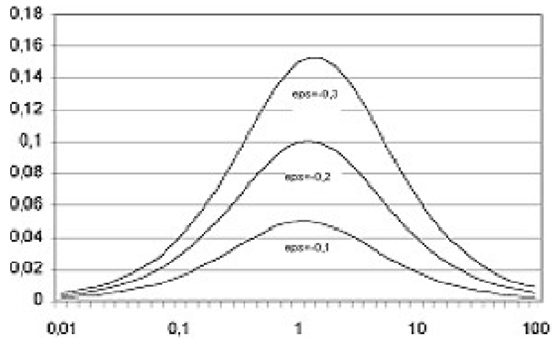

Figure 12. Efficiency diffuser valves: φ_{tot} *vs.* β.

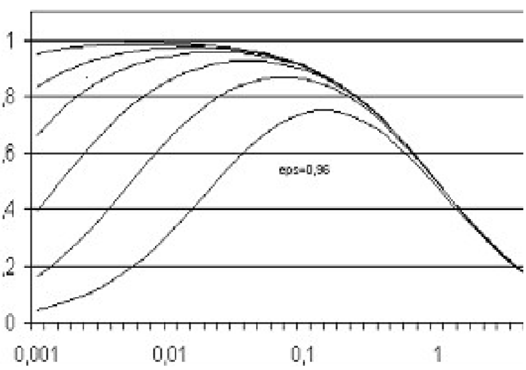

Figure 13. Efficiency valves cantilever: φ_{tot} *vs.* β'.

Table 4. Biomedical specifications.

Element	Values	
Pressure	> 60 kPa	no bubbles
Inlet pressure	1360 kPa	inner body
Inlet tube	diameter = 1.2 mm	Length = 12 cm
Outlet tube	diameter = 5 mm	Length = 50 cm
Flow-rate	2 ml/s	typical
Dimensions	2–3 cm	Max

As previously mentioned, the aim of this work was to design a micropump suitable for a biomedical application in which the following specifications (table 4) could be satisfied.

Applying the considerations made so far to both micropump designs reported in the literature, we have extracted an optimum parameter list that is shown in tables 5 and 6, for the micropump with diffuser valves and membrane valves, respectively. The corresponding simulated diagram of flow-rate as a function of the operating frequency is reported in figures 14 and 15, respectively.

Table 5. Optimized pump parameters (diffuser valves).

Elements	Symbol	Value
Membrane radius	a	10 mm
Membrane thickness	h	0.38 mm
Actuator radius	A_{act}	8 mm
Pump chamber radius	r	10 mm
Valves length	L	11.34 mm
Minimum diameter valves	$h_v(0)$, $w_v(0)$	0.405 mm
Average diameter valves	h_m, h_m	0.483 mm

Table 6. Optimized pump parameter (membrane valves).

Elements	Symbol	Value
Membrane radius	a	10 mm
Membrane thickness	h	0.42 mm
Actuator radius	A_{act}	8 mm
Actuator thickness	h	0.5 mm
Pump chamber vol.	V_c	0.36 µl
Valves radius	r	6.25 mm

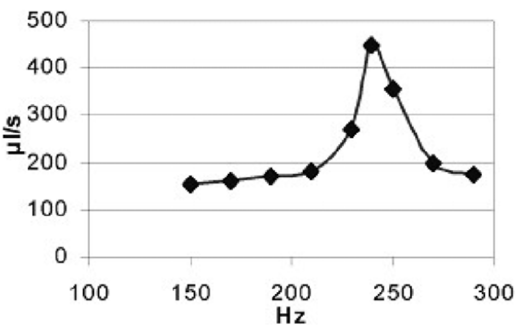

Figure 14. Flow-rate optimized for micropump with diffuser valves.

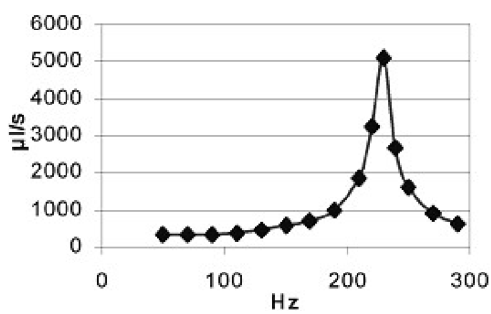

Figure 15. Flow-rate optimized for micropump with membrane valves.

4. Conclusion

The description of a microfluidic system through the parameters of an equivalent electrical circuit is valid to a first approximation even though a great part of the non-linear behaviour of the system components is neglected. In spite of this, the simulation results are satisfactory when compared with the published experimental data.

Starting from the analysis of two basic micropump designs, we have shown that an important condition for optimum performance is a suitable impedance matching between the valves and the tubes.

The efficiency of a micropump with diffuser valves is about ten times lower than that of a micropump with cantilever valves, so it does not succeed in matching the demanded high flow-rate. On the contrary, the cantilever micropump can approach a theoretical maximum flow rate of about $5.0\,\mathrm{mL\,s^{-1}}$.

From the data reported in table 5, valve sizes are much bigger compared to those found in the literature. Another solution used to reduce valve resistivity and improve the system performance is to substitute a large valve with an array of small valves.

An accurate, further analysis of non-linear effects is necessary in order to validate these results completely. A finite element simulation of the electromechanical behaviour of the entire device with the ANSYS software is in progress and is leading us to good results. An analysis of the fluid-dynamic behaviour of the valves is also allowing us to obtain realistic values of the components to be used in the SPICE simulations presented in this article.

From a technological point of view, there are two different possibilities to obtain non-mechanical valves. Isotropic etching techniques allow us to obtain the diffuser valves presented in this article. Nozzle valve behaviour is similar to that of diffuser valves. They have an interior performance in terms of efficiency, but can be obtained more easily with anisotropic etching techniques that allow us to use a shorter space and make the device smaller.

The micropumps we have presented are optimized to be used in the treatment of Hydrocephalus. However, the flexibility in the choice of constitutive elements allows us to use this device in various fields of interest.

In fact it is possible to drive the actuator according to signals coming from different sensors; the diameter of the valves, the dimension of the pump chamber and the characteristics of the membrane can be modified in order to properly handle the liquid.

References

[1] S. Bohm, W. Olthuis, P. Bergveld. *Sens. Act.*, **77**, 223 (1999).
[2] A. Ullmann, I. Fono. *J. Micro-electromech. Sys.*, **11**, 655 (2002).
[3] T. Bourouina, J.P. Grandchamp. *J. Micromech. Microeng.*, **6**, 398 (1996).
[4] R.E. Oosterbroek. Modeling, design and realization of microfluidic components. PhD thesis, University of Twente, MESA Research Institute (1999).
[5] J. Qian, Y. Zhao. *Mater. Design*, **23**, 619 (2002).
[6] T. Gerlach. *Sens. Act.*, **A69**, 181 (1998).